ChemComm

Facet-Dependent Acidic and Catalytic Properties of Sulfated Titania Solid Superacids

Journal:	*ChemComm*
Manuscript ID:	CC-COM-06-2015-004548.R1
Article Type:	Communication
Date Submitted by the Author:	16-Jul-2015

Complete List of Authors:	Hu, Yichen; Fudan University, Chemistry Guo, Bin; Fudan University, Chemistry Fu, Yingyi; Fudan University, Chemistry Ren, Yuanhang; Fudan University, Chemistry Tang, Gangfeng; Fudan University, Chemistry Chen, Xueying; Fudan University, Chemistry Yue, Bin; Fudan University, Chemistry He, Heyong; Fudan University, Chemistry

ChemComm

RSCPublishing

COMMUNICATION

Facet-Dependent Acidic and Catalytic Properties of Sulfated Titania Solid Superacids

Cite this: DOI: 10.1039/x0xx00000x

Yichen Hu, Bin Guo, Yingyi Fu, Yuanhang Ren, Gangfeng Tang, Xueying Chen, Bin Yue*, and Heyong He*

Received 00th January 2012,
Accepted 00th January 2012

DOI: 10.1039/x0xx00000x

www.rsc.org/

Sulfated titania solid superacids with dominant {001}, {001}/{101}, and {101} facets were prepared by the hydrothermal method and subsequent sulfation. Their facet-dependent acidic properties were investigated by the solid-state ^{31}P NMR technique and Pechmann condensation of 5,7-dihydroxy-4-methyl coumarin.

Surface atomic structure significantly influences the catalytic activity of various metal oxide nanomaterials.[1,2] Hence, morphological control of nanocrystals with exposed distinct crystal facets is vital in the design and application of metal oxides as catalysts. For instance, the facet-dependent catalytic activity of anatase TiO_2 has been intensively investigated.[3] High-energy facets of anatase titania such as {001},[4] {100},[5] {103}[6] and {105}[7] were successfully prepared. In particular, anatase TiO_2 with dominant {001} facets has attracted enormous attention with its enhanced performance in photo-catalysis,[4] dye-sensitized solar cells[8] and lithium ion batteries.[9] Another aspect of research about metal oxides has focused on the sulfated metal oxide (SO_4^{2-}/ZrO_2,[10] SO_4^{2-}/SnO_2,[11] SO_4^{2-}/TiO_2,[12] *etc.*) which emerges as solid superacid catalysts. Compared with conventional homogeneous acid catalysts such as H_2SO_4, HF and H_3PO_4, solid superacid heterogeneous catalysts possess the advantage of facile separation from the reaction mixture, which is in favor of regeneration and reutilization of catalysts without bringing about the problem of waste disposal. The application of sulfated metal oxide catalysts have been achieved in isomerization, alkylation, esterification, acylation, *etc*.[13-15] Amongst the metal oxide based solid superacid catalysts, sulfated titania plays an important role due to its biological and chemical inertness, high catalytic activity and low cost. The acid sites on sulfated metal oxides are induced by the bonding of two oxygen atoms from SO_4^{2-} group to metal atom. Thus, the electron-withdrawing S=O covalent bond induces metal atoms to manifest electron-deficiency, forming Lewis acid sites. The acidic proton derived from the surface hydroxyl group of metal oxides linked to the Lewis acid site can be easily released to introduce Brønsted acid site. Generally the acid strength is influenced by the electronegativity, valence and coordination numbers of metal atoms. Hence the acid strength of sulfated metal oxides is determined by the surface atomic configuration.[16] As the surface structure of different facet exposed TiO_2 is dissimilar, their superacid property is deduced to be different. Therefore, it is highly desirable to investigate the relationship between acidic properties of sulfated TiO_2 and dominant facets of TiO_2.

In the present work, we report the preparation of sulfated TiO_2 solid superacid catalyst with dominant {001} facets *via* hydrothermal reaction followed by surface sulfate modification. Sulfated TiO_2 with approximately equal percentage of {001} and {101} facets, as well as conventional sulfated TiO_2 with dominant {101} facets were also prepared through the same procedure for comparison. The acid properties of as-prepared catalysts were studied by ^{31}P MAS NMR spectroscopy with trimethylphosphine (TMP) as the probe molecule. The Pechmann reaction of phloroglucinol with ethyl acetoacetate under solvent-free condition was carried out to assess the activity of the catalysts. The products of this reaction, coumarin derivatives, are important substances in synthetic organic chemistry.[17]

Titania sample with dominant {001} facets was prepared by a hydrothermal reaction of $Ti(OC_4H_9)_4$ (5 ml) and hydrofluoric acid (40~48 wt.%, 0.6 ml), which was subsequently treated with $(NH_4)_2SO_4$ to obtain sulfated TiO_2 solid superacid catalyst (noted as ST_{001}). When the amount of HF was reduced to 0.2 ml, the ratio of exposed {001} facets versus {101} facets was tuned to be approximately 1:1 (noted as $ST_{001/101}$). Furthermore, conventional sulfated titania was also prepared through the same procedure without HF (noted as ST_{101}). The detailed synthesis procedures are shown in ESI. The powder X-ray diffraction (XRD) patterns shown in Fig. 1a reveal that all these samples display characteristic peaks of anatase TiO_2 (PDF 21-1272, tetragonal, space group: $I4_1/amd$). The broadening of the (004) peak of ST_{001} compared with $ST_{001/101}$ and ST_{101} indicates a decrease of the crystallite size in the direction perpendicular to {001} facets. The transmission electron microscopy (TEM) image of ST_{001} in Fig. 1b shows that the ST_{001} sample consists of nanosheets with a shape of truncated octahedral bipyramid. A HRTEM image (Fig. 1c) of the side view exhibits clear lattice fringes with *d* spacing of 0.347 and 0.465 nm, in accordance with (101) and (002) planes of anatase TiO_2, respectively. The average side length and thickness of ST_{001} nanosheets is measured to be about 50 nm and 6 nm, respectively, without obvious change

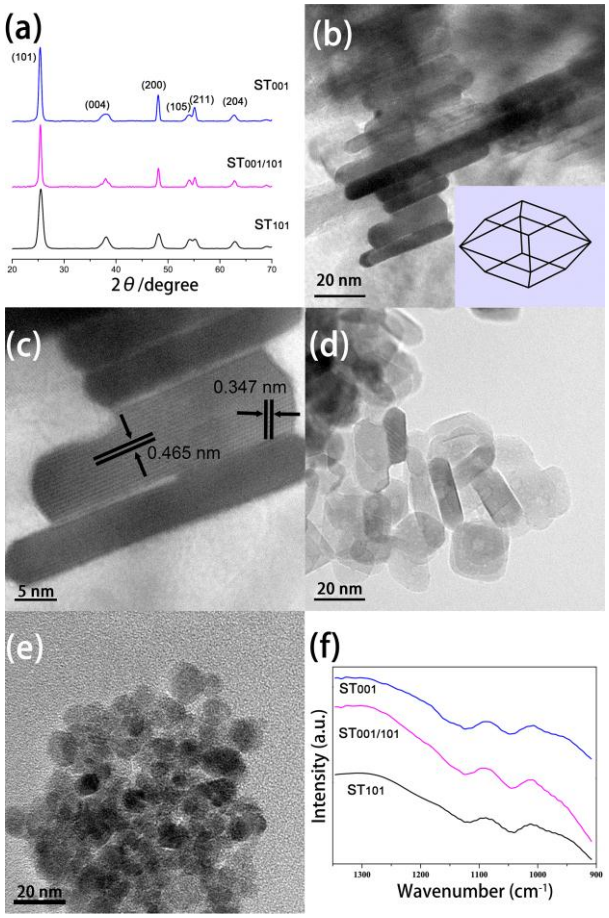

Fig. 1 (a) XRD patterns of ST_{001}, $ST_{001/101}$ and ST_{101}, (b) TEM image of ST_{001}, inset is the theoretical model of sulfated titania nanosheets, (c) HRTEM image of ST_{001}, (d) TEM image of $ST_{001/101}$, (e) TEM image of $ST_{101;}$ (f) FT-IR spectra of ST_{001}, $ST_{001/101}$ and ST_{101}.

compared with the parent TiO_2 nanosheets[18] (ESI, Fig. S1 and Fig. S2). The percentage of exposed {001} and {101} facets is, therefore, estimated to be 80% and 20%, respectively (Fig. S3). The side length and thickness of $ST_{001/101}$ nanosheets (Fig. 1d) is estimated as *ca.* 25 nm and 10 nm, respectively, hence the percentages of {001} and {101} facets are estimated to be 54% and 46%, respectively. ST_{101} (Fig. 1e) consists of aggregated ellipsoid nanoparticles with the size of *ca.* 10 nm and the percentage of exposed {001} is estimated less than 10%.[19] The physico-chemical properties of ST_{001}, $ST_{001/101}$ and ST_{101} are summarized in Table S1. The BET surface area of ST_{001} is lower than that of $ST_{001/101}$ and ST_{101}, which matches well with the fact that ST_{001} possesses a larger crystallite size. In Fig. 1f, FT-IR spectra of ST_{001}, $ST_{001/101}$ and ST_{101} show two bands in the region of 1200-900 cm^{-1}, with two peaks at 1128 and 1048 cm^{-1} assigned to symmetric and asymmetric S=O vibration frequency,[20] respectively. These are the characteristic frequencies of inorganic chelating bidentate sulfate coordinated to Ti atoms, suggesting the successful sulfation of titania. Elemental analysis results indicate that the amount of sulfate in the three sulfated titania catalysts is almost the same (Table S1).

Solid state NMR spectroscopy is a powerful tool for the measurement of solid acidity.[21,22] Compared with other commonly used solid acidity characterization techniques, such as temperature programmed desorption of ammonia and FT-IR spectroscopy of pyridine, solid state NMR has been shown to be

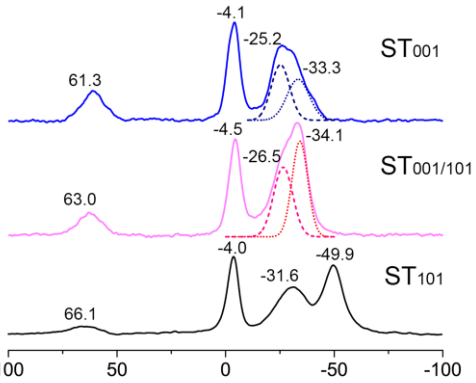

Fig. 2 ^{31}P MAS NMR spectra of TMP loaded on ST_{001}, $ST_{001/101}$ and ST_{101}. The dashed curves indicate results of spectral deconvolution.

sensitive and reliable in terms of providing abundant information on the acid type, acid strength, and strength distribution in various solid acids. TMP is a widely used probe molecule for detecting acid properties of solid acid catalysts.[22,23] TMP molecules bound to Lewis acid sites give rise to ^{31}P resonances in the range from -30 to -60 ppm. While adsorbing on Brønsted acid sites, TMP molecules are subsequently protonated to form $TMPH^+$, bringing the ^{31}P resonances in the range of 0 to -5 ppm. The ^{31}P MAS NMR spectra of TMP adsorbed on ST_{001}, $ST_{001/101}$ and ST_{101} are presented in Fig. 2. In ST_{101}, four peaks at 66.1, -4.0, -31.6, and -49.9 ppm are observed. The two peaks located in the range between -30 and -60 ppm are ascribed to TMP coordinated with Lewis acid, implying the existence of two distinct Lewis acid sites. The peak at -4.0 ppm is assigned to $TMPH^+$ raised from the protonation of TMP. In addition, the broad peak at 66.1 ppm can be assigned to trimethylphosphine oxide (TMPO) bound to the acid sites. The formation of TMPO is due to the oxidation of TMP on the surface of sulfated titania.[24] In the ^{31}P MAS NMR spectrum of TMP adsorbed on $ST_{001/101}$, the chemical shift related to TMPO and Brønsted acid sites remains while the peak attributed to Lewis acid sites appears at -26.5 and -34.1 ppm, suggesting the increase in Lewis acid strength. As for TMP adsorbed on ST_{001}, the peak related to TMPO and Brønsted acid sites appear at 61.3 and -4.1 ppm, respectively. However, the peaks induced by the interaction of TMP with Lewis acid sites further shift to -25.2 and -33.3 ppm. Therefore, the ^{31}P MAS NMR results demonstrate that the sulfated TiO_2 solid superacid catalyst

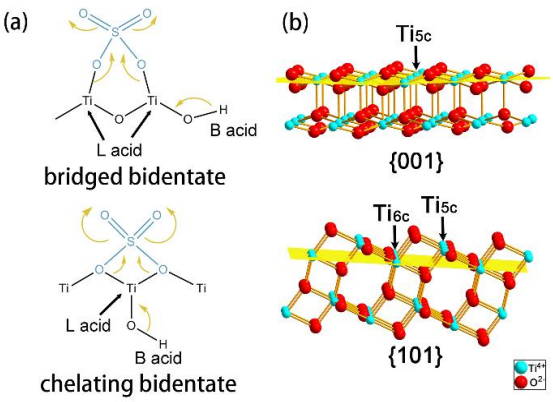

Fig. 3 (a) Proposed bonding modes of sulfated TiO_2, (b) Schematic atomic structure of {001} and {101} facets of anatase TiO_2.

Table 1 Acid properties of sulfated titania samples

Sample	Acid type	Chemical shift (ppm)	Acid density [a] (μmol·m^{-2})	Total acid density [a] (μmol·m^{-2})	Ti_{5c} atoms on (001) facet (μmol·m^{-2}) [b]	Ti_{5c} atoms on (101) facet (μmol·m^{-2}) [b]	Total Ti_{5c} atoms (μmol·m^{-2}) [b]
ST_{001}	Brønsted	-4.1	1.36				
	Lewis	-33.3, -25.2	1.16, 1.18	4.36	9.20	1.68	10.88
	TMPO	61.3	0.66				
$ST_{001/101}$	Brønsted	-4.5	1.08				
	Lewis	-34.1, -26.5	1.42, 1.21	4.12	6.21	3.86	10.07
	TMPO	63.0	0.41				
ST_{101}	Brønsted	-4.0	1.20				
	Lewis	-49.9, -31.6	1.87, 1.73	5.06	1.15 [c]	7.56 [c]	8.71 [c]
	TMPO	66.1	0.26				

[a] The density of acid sites with different chemical shifts are derived using the re-normalized relative concentrations obtained from spectral simulation by Gaussian deconvolution with $NH_4H_2PO_4$ as the reference.
[b] Density of total Ti_{5c} atoms = Percentage of {001} facets × Ti_{5c} atoms on (001) facet + Percentage of {101} facets × Ti_{5c} atoms on (101) facet.[25]
[c] The percentage of {001} facets and {101} facets are taken as 90% and 10%, respectively.

with dominant {001} facets, *i.e.*, ST_{001}, is endowed with the highest Lewis acid strength. The enhancement of Lewis acid strength with the increase of percentage of exposed {001} facets derives from the concept of Lewis acid. Lewis acids are defined as electron-deficient molecules or ions. It is generally assumed that coordinatively unsaturated titanium sites function as the Lewis acid sites on sulfated titania and the interaction between the hydroxyl groups and the Lewis acid sites generates Brønsted acid sites (Fig. 3a). Fig. 3b shows the atomic structure model of {001} and {101} facets of anatase TiO_2. {101} facets of anatase TiO_2 have 50% saturated six-coordinated Ti atoms (Ti_{6c}) and 50% unsaturated five-coordinated Ti atoms (Ti_{5c}) while {001} facets consist of 100% Ti_{5c} atoms.[26] Therefore, sulfated titania with selectively exposed {001} facets, which apparently possesses more unsaturated metal atoms as Lewis acid sites, favors the enhancement of Lewis acid concentration. In addition, based on surface area data, the density of acid sites including both Brønsted and Lewis acid is also obtained. The ratio of total acid concentration in ST_{001} (4.36 μmol·m^{-2}) against $ST_{001/101}$ (4.12 μmol·m^{-2}) is 1.06 (Table 2), which is in accordance with the value calculated from the surface concentration of Lewis acid sites on aforementioned facets (10.88 : 10.07 = 1.08).[25] The abnormal high acid concentration of ST_{101} is speculated to be related with its irregular shape which leads to more possibilities of interacting with $(NH_4)_2SO_4$ to introduce acid sites.

The catalytic performances of ST_{001}, $ST_{001/101}$ and ST_{101} in Pechmann condensation using phloroglucinol and ethyl acetoacetate as starting reagents are shown in Fig. 4. The yield of 5,7-dihydroxy-4-methyl coumarin is in the order of ST_{001} > $ST_{001/101}$ > ST_{101}. The result shows that {001} facets selectively exposed sulfated titania exhibited the highest catalytic activity. In view of Pechmann reaction, the condensation of phenol and *β*-keto ester proceeds through transesterification followed by intramolecular hydroalkylation and dehydration, which can be catalyzed by both Brønsted and Lewis acids.[27] In Table 1 the NMR results indicate that the catalytic activity is not mainly related to Brønsted or Lewis acid density. In fact the catalytic activity is generally consistent with the Lewis acid strength of the catalyst used. ST_{001} with the largest percentage of exposed {001} facets exhibits the strongest Lewis acid strength as unveiled in ^{31}P MAS NMR analysis, leading to its highest catalytic activity.

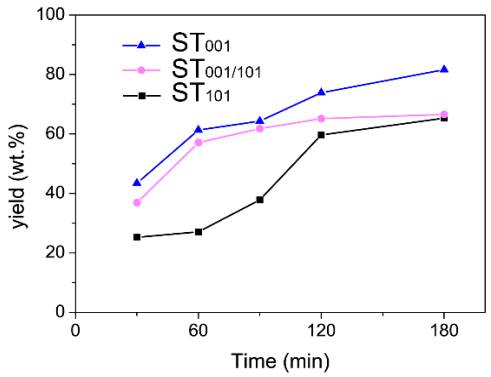

Fig. 4 Yield of 5,7-dihydroxy-4-methyl coumarin over ST_{001} (▲) $ST_{001/101}$ (●) and ST_{101} (■).

In conclusion, sulfated titania solid superacid catalysts with dominant {001}, {001}/{101} and {101} facets were prepared by a simple hydrothermal method and subsequent sulfation. Solid state NMR results indicated that ST_{001} was superior in Lewis acid strength to $ST_{001/101}$ and ST_{101}, due to the fact that {001} facet is constituted of entire unsaturated five-coordinated Ti atoms, beneficial to the formation of superacid. Consequently, the sulfated titania with dominant {001} facets appears to be more active in the synthesis of 5,7-dihydroxy-4-methyl coumarin under solvent-free condition through Pechmann condensation. This work provides a new route towards the study of structure sensitivity of solid acid catalysts and may inspire a better strategy in design of solid acid catalysts from the crystal morphology perspective.

Acknowledgement This work was supported by the National Natural Science Foundation (21371035, 21173050) and SINOPEC (X514005).

Notes and references

Department of Chemistry and Shanghai Key Laboratory of Molecular Catalysis and Innovative Materials, Collaborative Innovation Center of Chemistry for Energy Materials, Fudan University, Shanghai 200433, P.

R. China. E-mails: yuebin@fudan.edu.cn and heyonghe@fudan.edu.cn; Tel.: 0086-21-65643916; Fax: 0086-21-55665572

† Electronic Supplementary Information (ESI) available: [The details of synthesis, characterization and catalytic activity test reactions, N_2 adsorption-desorption isotherms, the calculation of percentage of {001} facets, proposed mechanism of reaction]. See DOI: 10.1039/c000000x/

1. Y. G. Sun and Y. N. Xia, *Science*, 2002, **298**, 2176-2179.
2. N. Tian, Z. Y. Zhou, S. G. Sun, Y. Ding and Z. L. Wang, *Science*, 2007, **316**, 732-735.
3. G. Liu, H. G. Yang, J. Pan, Y. Q. Yang, G. Q. Lu and H. M. Cheng, *Chem. Rev.*, 2014, **114**, 9559-9612.
4. X. G. Han, Q. Kuang, M. S. Jin, Z. X. Xie and L. S. Zheng, *J. Am. Chem. Soc.*, 2009, **131**, 3152-3153.
5. J. M. Li and D. S. Xu, *Chem. Commun.*, 2010, **46**, 2301-2303.
6. X. G. Han, B. J. Zheng, J. J. Ouyang, X. Wang, Q. Kuang, Y. Q. Jiang, Z. X. Xie and L. S. Zheng, *Chem. Asian J.*, 2012, **7**, 2538-2542.
7. H. B. Jiang, Q. Cuan, C. Z. Wen, J. Xing, D. Wu, X. Q. Gong, C. Z. Li and H. G. Yang, *Angew. Chem. Int. Ed.*, 2011, **50**, 3764-3768.
8. X. Wu, Z. G. Chen, G. Q. Lu and L. Z. Wang, *Adv. Funct. Mater.*, 2011, **21**, 4167-4172.
9. J. S. Chen, Y. L. Tan, C. M. Li, Y. L. Cheah, D. Y. Luan, S. Madhavi, F. Y. C. Boey, L. A. Archer and X. W. Lou, *J. Am. Chem. Soc.*, 2010, **132**, 6124-6130.
10. X. M. Song and A. Sayari, *Catal. Rev. Sci. Eng.*, 1996, **38**, 329-412.
11. A. S. Khder, E. A. El-Sharkawy, S. A. El-Hakam and A. I. Ahmed, *Catal. Commun.*, 2008, **9**, 769-777.
12. J. L. Ropero-Vega, A. Aldana-Perez, R. Gomez and M. E. Nino-Gomez, *Appl. Catal., A*, 2010, **379**, 24-29.
13. A. Corma, A. Martinez and C. Martinez, *Appl. Catal., A*, 1996, **144**, 249-268.
14. K. Arata, *Green Chem.*, 2009, **11**, 1719-1728.
15. G. D. Yadav and A. D. Murkute, *J. Catal.*, 2004, **224**, 218-223.
16. H. Zhao, P. P. Jiang, Y. M. Dong, M. Huang, and B. L. Liu, *New J. Chem.*, 2014, **38**, 4541-4548.
17. G. D. Yadav, N. P. Ajgaonkar and A. Varma, *J. Catal.*, 2012, **292**, 99-110.
18. Y. C. Hu, Y. H. Ren, G. F. Tang, C. Wang, M. Tang, B. Yue and H. Y. He, *Chin. J. Chem.*, 2014, **32**, 1151-1156.
19. Q. J. Xiang, K. L. Lv and J. G. Yu, *Appl. Catal., B*, 2010, **96**, 557-564.
20. T. Yamaguchi, T. Jin and K. Tanabe, *J. Phys. Chem.*, 1986, **90**, 3148-3152.
21. L. Zhang, Y. H. Ren, B. Yue and H. Y. He, *Chem. Commun.*, 2012, **48**, 2370-2384.
22. A. M. Zheng, S. J. Huang, S. B. Liu and F. Deng, *Phys. Chem. Chem. Phys.*, 2011, **13**, 14889-14901.
23. J. H. Lunsford, W. P. Rothwell and W. Shen, *J. Am. Chem. Soc.*, 1985, **107**, 1540-1547.
24. J. F. Haw, J. H. Zhang, K. Shimizu, T. N. Venkatraman, D. P. Luigi, W. G. Song, D. H. Barich and J. B. Nicholas, *J. Am. Chem. Soc.*, 2000, **122**, 12561-12570.
25. C. Arrouvel, M. Digne, M. Breysse, H. Toulhoat and P. Raybaud, *J. Catal.*, 2004, **222**, 152-166.
26. J. Pan, G. Liu, G. M. Lu and H. M. Cheng, *Angew. Chem. Int. Ed.*, 2011, **50**, 2133-2137.
27. S. Sudha, K. Venkatachalam, S. V. Priya, J. H. Mabel, M. Palanichamy and V. Murugesan, *J. Mol. Catal. A: Chem.*, 2008, **291**, 22-29.

